Niche cells spatially restrict stem-cell self-renewal signaling via receptor-ligand degradation

Sophia Ladyzhets[1], Taylor Simao[1] Matthew Antel[1] and Mayu Inaba[1, *]

1. Department of Cell Biology, University of Connecticut Health Center, Farmington, CT 06030

[*] Correspondence: inaba@uchc.edu

`

Abstract

Stem-cell niche signaling is short-range in nature, such that only stem cells and not their differentiating progeny experience self-renewing signals[1]. At the apical tip of the *Drosophila* testes, 8 to 10 germline stem cells (GSCs) surround the hub, the niche signaling center. Microtubule-based nanotubes (MT-nanotubes) formed by GSCs project into the hub cells, serves as the platform for niche signal reception. Here we show that the receptor for Decapentaplegic (Dpp) accumulated on MT-nanotubes is internalized into hub cells together with the Dpp ligand, and both are degraded in the hub cell lysosomes. Perturbation of hub lysosomal function or MT-nanotube formation lead to excess receptor retention within GSCs as well as excess Dpp ligand that diffuses out of the hub. Our results indicate that degradation of the self-renewal ligand/receptor by niche cells specially restrict the niche signal range, and that might be a general feature of stem-cell niche signaling.

Introduction

Many stem cells are known to reside in a special microenvironment known as the niche to maintain their identity. *Drosophila* male GSCs typically divide asymmetrically within the niche. The daughter cell attached to the hub self-renews, while the daughter displaced from the hub initiates differentiation program[2,3-4]. The receptor, Thickveins (Tkv), is produced by GSCs and trafficked to the surface of MT-nanotubes, which protrude into the hub cells. At the surface of the MT-nanotubes, Tkv interacts with the ligand, Dpp which is secreted from the hub cells, resulting in activation/phosphorylation of the downstream protein Mothers against dpp (Mad) in GSCs[5]. (Figure 1A). Previously, we have shown that Tkv-GFP is not seen in the cell body of GSCs when expressed in GSCs. Instead, Tkv-GFP is trafficked to the MT-nanotubes and thus only observed in hub area

(Figure S1A, B), indicating that there must be the mechanism to restrict Tkv localization/amount to be exclusively on the MT-nanotubes so that receptor/ligand interaction only occurs at the MT-nanotube membrane.

Results

To understand/follow the fate of the Tkv receptor, we monitored fully functional Tkv transgenes expressed in germline cells. We first induced GSC clones co-expressing Tkv–mCherry and GFP–αTub. Tkv was seen along the MT-nanotubes and within hub cells in the small spots (punctae) vicinity of the clone (Figure 1B). Tkv positive punctae in the hub cells were colocalized with lysotracker (Figure 1C) and lysosomal-associated membrane protein-1 fused to GFP (Lamp1-GFP[6]; Figure 1D), revealing that Tkv expressed in GSC localizes to lysosomes in hub cells. Colocalization was observed in a Tkv protein-trap line in which endogenous Tkv protein was fused to YFP[7], indicating that the lysosomal localization was not an artifact of over-expression (Figure 1E). The typeII receptor Punt, which forms a heterodimer with Tkv (Figure 1F, Figure S2D)[2 8 9] likely upon the ligand binding[10], was observed in the hub lysosomes. We have previously demonstrated that the Dpp ligand and Tkv expressed from GSC interacts on MT-nanotubes thus observed in the hub area[5]. The Dpp ligand seen in the punatae in the hub (Figure 1G) was also colocalized to the hub lysosomes, suggesting that the ligand-receptor complex is the target of degradation. Consistently, a reporter of ligand-bound Tkv, TIPF[11] was also observed in the hub cell lysosomes (Figure 1H). These observations suggest that Tkv protein is being internalized into hub cells for lysosomal degradation and that Tkv might be downregulated upon signal reception.

To investigate the function of Tkv degradation in hub lysosomes, we inhibited lysosomal-dependent degradation using chloroquine (CQ), a drug that raises lysosomal pH and inhibits lysosomal enzymes[12–14]. CQ treatment of isolated testes substantially increased the amount of Tkv within the hub lysosomes (Figure 2A-F). Moreover, we sometimes observed that Tkv was present on the surface of GSC cell body (Figure 2B, E, red arrows, Table1), suggesting that Tkv degradation in the hub limits the amount of Tkv in GSCs. The Tkv retention within GSC plasma membrane seen in the presence of CQ was similar to that seen in MT-nanotube defective (knocked down of three IFT-B; Intraflagellar transport-B genes) GSCs (Figure S1C and D, Table1)[5] or Dpp ts mutant background, which also causes MT-nanotube defect (Figure S1E and F), indicating that Tkv might be trafficked via MT-nanotube into hub lysosomes. There is the possibility that some extent of Tkv degradation is occurring in GSC itself as we observed small amount of Tkv signal in punctae within GSC (black

arrowheads in Figure 2A, B, E and D). However, CQ treatment of Tkv-YFP protein trap testis showed clear Tkv accumulation in the lysosomes in the hub and later stage spermatocytes (Figure S2B, cells distal from hub, B'), indicating that Tkv degradation in GSCs and their immediate progeny are minimum level. Therefore, we conclude that majority of Tkv protein in GSC is degraded in hub cells.

To examine the consequence of defective Tkv degradation on downstream signaling, testes from CQ-fed males were labelled for pMad, an indicator of Dpp signal activation (Figure 2G, H and I). CQ-mediated lysosomal inhibition increased pMad levels in GSCs. Overall, these data suggest that Tkv's transport to the hub lysosomes is mediated by MT-nanotubes, and further indicate that Tkv degradation in the hub lysosome is essential for reducing the niche signal.

To determine whether the lysosomes originate in the hub or germ cells, genes involved in lysosomal-dependent degradation were knocked down using hub- and/or germ cell-specific GAL4 drivers. Spinster (Spin) is a lysosomal H^+-carbohydrate transporter and a known regulator of lysosomal biogenesis, as well as a regulator of Dpp signaling[15,16]. Lamp1 is an abundant protein in the lysosomal membrane that is required for lysosomes to fuse with endosomes/autophagosomes[17]. Germ cell-specific knockdown of these genes did not alter pMad level (Figure 3A-D and I). In contrast, hub-specific down-regulation of these genes led to a significant increase in pMad level in GSCs and their immediate progeny (Figure 3E-H and I), as well as an increased in the size of Tkv puncta in the hub (Figure 3J-M and N, Table1), indicating that impaired Tkv digestion in hub lysosomes enhanced the niche signal. *dpp* mRNA levels showed no detectible alteration in lysosomal-defective hub cells (Figure S3), indicating that regulation of the *dpp* signal by hub cell lysosomes is not caused by a change in niche ligand production at the transcriptional level.

Ubiquitination of membrane proteins is required for recognition by the endosomal sorting complexes required for transport, and thence endocytosis, lysosomal fusion and degradation[18]. SMAD ubiquitination regulatory factor (Smurf)-mediated Tkv ubiquitination is necessary for GSC differentiation both in testicular and ovarian GSCs[19,20]. Smurf is a HECT (Homologous to the E6-AP Carboxyl Terminus) domain containing protein with E3 ubiquitin ligase activity, and disruption of Smurf function enhances Dpp-Tkv signal activation[20]. It has been reported that Tkv Ser238 residue phosphorylation is required for Smurf dependent ubiquitination[19]. To determine if ubiquitination-defective Tkv no longer localizes to hub cells we mutated the Ser 238 phosphorylation site to alanine. Unlike wild-type Tkv-GFP, which localized to the hub lysosomes, Tkv-S238A-GFP was predominantly localized to the GSC cell body along plasma membrane. Although Tkv-S238A-GFP

illuminates MT-nanotubes (thread-like pattern) in the hub, typical lysosome localization pattern (round punctae-like pattern) dominated in control testis was barely observed, indicating that ubiquitination is critical for Tkv's translocation into hub lysosomes (Figure 3O and P, Table1). Expression of Tkv-S238A-GFP in the GSC resulted in elevated signal activation as indicated by higher pMad levels (Figure 3Q, R and S). Thus, Tkv protein is the target of lysosomal degradation in hub cells, allowing hub lysosomes to negatively regulate Dpp signaling.

Since Dpp ligand also localizes to hub lysosomes (Figure 1G), we hypothesized that Dpp may be also degraded there. To test this idea, we expressed Dpp-mCherry fusion protein specifically in hub cells using the hub specific GAL4 driver. mCherry signal was only observed within the hub, and no signal was detected outside the hub (Figure 4A). CQ treatment of the testis to impair lysosome function increased the size of Dpp-mCherry positive punctae within hub cells as seen for Tkv (Figure 4B, C). We also detected abundant Dpp-mCherry signal outside the hub after a 2 hour-treatment (Figure 4B, D). Similar results were obtained by using a Dpp-GFP line carrying a fosmid genomic construct in which Dpp has been fused to GFP[21] (Figure S4). These data support the idea that Dpp is also degraded in hub lysosomes. Furthermore, after 4 hour-CQ treatment, we also detected TIPF (a reporter of ligand-bound Tkv) in broad area outside of the hub, consistent with the idea of Dpp diffusion (Figure 4E, F).

To determine if Dpp-mCherry detected outside the hub is due to its free diffusion into the extracellular space, we used fluorescence recovery after photobleaching (FRAP) analysis. After photobleaching, the recovery was rapid with an average time to reach to 50% of the original intensity, 8.2 ± 2.2 seconds (n=6) (Figure 4G, H, movie3, 4). Signal did not fully recover indicating the possible existence of bleached background caused by autofluorescence or the possibility that some Dpp protein might be trapped likely binding to the extracellular matrix components in photobleached field as reported in *Drosophila* embryo[22]. The Dpp-mCherry signal in lysosomes within the hub did not recover quickly after photobleaching (movie5, no recovery was seen up to 30 min monitoring, n=10 experiments) as seen in the areas outside of the hub when bleached. These data suggest that in the absence of proteolysis Dpp ligand can diffuse from the hub, and that MT-nanotubes and lysosome activity prevent it from doing so.

Discussion

We have shown previously that niche cells and stem cells interact in a contact-dependent manner, with GSCs and the hub cells engaging in productive signaling via MT-nanotubes, enabling

highly specific cell-cell interactions and excluding non-stem cells from receiving the stem cell signals. Here, we demonstrate that lysosomes in the niche cells, also through MT-nanotube interactions, degrade both the ligand from the niche, its receptor from the stem cell, thus dampening stem-cell renewal signaling (Figure 4I). This ensures the removal of signaling molecules and further prevents "contact-independent" ligand-receptor interactions outside of the niche. Indeed, lysosomal localization-defective Tkv (S238A), and MT-nanotube loss, both cause elevated Tkv levels within GSCs, and MT-nanotube loss also induces Dpp ligand diffusion in the *Drosophila* testis. Proteolysis manipulation in our study changed the localization of Tkv from one place to the other (in the Hub lysosomes or GSC plasma membrane, Table1), suggesting that there may be two steps of this regulation, first, Tkv trafficking into hub cells, second; Tkv degradation in hub lysosomes. We examined here Spin and Lamp1, likely regulating the terminal step within lysosomes. Identification of more regulators will help to understand entire molecular mechanism. Cytonemes, another type of actin-dependent signaling protrusion [23] [24], also transfer ligand and receptor, allowing the interaction between cells at a distance. Ligand-producing and receptor-producing cells both form cytonemes and both cells have been observed to take up signaling proteins: receptor into the ligand-producing cells and ligand into the receptor-producing cells[24], indicating the universality of such transfer in general contact-dependent signaling. It remains to be investigated whether lysosomal proteolysis of ligand and receptor, as demonstrated by our study, might also regulate signaling by cytonemes.

Acknowledgements

We thank Yukiko Yamashita, Helmut Krämer, Elizabeth R. Gavis, Thomas B. Kornberg, Saugata Roy, the Bloomington Drosophila Stock Center and the Developmental Studies Hybridoma Bank and the Vienna Drosophila Resource Center for reagents; Laurinda Jaffe, Michael Buszczak, Yukiko Yamashita and the Inaba laboratory members for discussion; Christopher Bonin for manuscript editing; this work was supported by an NIH grant 1R35GM128678-01 and start-up funds from UConn Health (to M.I.).

Author Contributions

M.I, Conception and design, acquisition of data, analysis and interpretation of data, drafting or revising the article; S.L, M.A, T.S, Acquisition of data, analysis and interpretation of data, drafting or revising the manuscript.

Declaration of Interests

The authors declare no competing interests.

References

1. Morrison, S. J. & Kimble, J. Asymmetric and symmetric stem-cell divisions in development and cancer. *Nature* **441**, 1068–1074 (2006).
2. Kawase, E., Wong, M. D., Ding, B. C. & Xie, T. Gbb/Bmp signaling is essential for maintaining germline stem cells and for repressing bam transcription in the Drosophila testis. *Development* **131**, 1365–75 (2004).
3. Tulina, N. & Matunis, E. Control of stem cell self-renewal in Drosophila spermatogenesis by JAK-STAT signaling. *Science* **294**, 2546–9 (2001).
4. Yamashita, Y. M., Jones, D. L. & Fuller, M. T. Orientation of asymmetric stem cell division by the APC tumor suppressor and centrosome. *Science.* **301**, 1547–1550 (2003).
5. Inaba, M., Buszczak, M. & Yamashita, Y. M. Nanotubes mediate niche-stem-cell signalling in the Drosophila testis. *Nature* **523**, 329–32 (2015).
6. Akbar, M. A., Ray, S. & Krämer, H. The SM Protein Car/Vps33A Regulates SNARE-mediated Trafficking to Lysosomes and Lysosome-related Organelles. *Mol. Biol. Cell* **20**, 1705–1714 (2009).
7. Yuva-Aydemir, Y., Bauke, A.-C. & Klämbt, C. Spinster controls Dpp signaling during glial migration in the Drosophila eye. *J. Neurosci.* **31**, 7005–15 (2011).
8. Ruberte, E., Marty, T., Nellen, D., Affolter, M. & Basler, K. An absolute requirement for both the type II and type I receptors, punt and thick veins, for Dpp signaling in vivo. *Cell* **80**, 889–897 (1995).
9. Letsou, A. *et al.* Drosophila Dpp signaling is mediated by the punt gene product: a dual ligand-binding type II receptor of the TGF beta receptor family. *Cell* **80**, 899–908 (1995).
10. Lin, H. Y. *et al.* The soluble exoplasmic domain of the type II transforming growth factor (TGF)-beta receptor. A heterogeneously glycosylated protein with high affinity and selectivity for TGF-beta ligands. *J. Biol. Chem.* **270**, 2747–54 (1995).
11. Michel, M., Raabe, I., Kupinski, A. P., Pérez-Palencia, R. & Bökel, C. Local BMP

receptor activation at adherens junctions in the Drosophila germline stem cell niche. *Nat. Commun.* **2**, 415 (2011).

12. Seglen, P. O., Grinde, B. & Solheim, A. E. Inhibition of the lysosomal pathway of protein degradation in isolated rat hepatocytes by ammonia, methylamine, chloroquine and leupeptin. *Eur. J. Biochem.* **95**, 215–25 (1979).
13. Poole, B. & Ohkuma, S. Effect of weak bases on the intralysosomal pH in mouse peritoneal macrophages. *J. Cell Biol.* **90**, 665–9 (1981).
14. Wibo, M. & Poole, B. Protein degradation in cultured cells. II. The uptake of chloroquine by rat fibroblasts and the inhibition of cellular protein degradation and cathepsin B1. *J. Cell Biol.* **63**, 430–40 (1974).
15. Sweeney, S. T. & Davis, G. W. Unrestricted synaptic growth in spinster-a late endosomal protein implicated in TGF-beta-mediated synaptic growth regulation. *Neuron* **36**, 403–16 (2002).
16. Yuva-Aydemir, Y., Bauke, A.-C. & Klambt, C. Spinster Controls Dpp Signaling during Glial Migration in the Drosophila Eye. *J. Neurosci.* **31**, 7005–7015 (2011).
17. Eskelinen, E.-L. Roles of LAMP-1 and LAMP-2 in lysosome biogenesis and autophagy. *Mol. Aspects Med.* **27**, 495–502 (2006).
18. Piper, R. C. & Lehner, P. J. Endosomal transport via ubiquitination. *Trends Cell Biol.* **21**, 647–655 (2011).
19. Xia, L. *et al.* The Fused/Smurf complex controls the fate of Drosophila germline stem cells by generating a gradient BMP response. *Cell* **143**, 978–90 (2010).
20. Chang, Y.-J., Pi, H., Hsieh, C.-C. & Fuller, M. T. Smurf-mediated differential proteolysis generates dynamic BMP signaling in germline stem cells during Drosophila testis development. *Dev. Biol.* **383**, 106–20 (2013).
21. Sarov, M. *et al.* A genome-wide resource for the analysis of protein localisation in Drosophila. *Elife* **5**, e12068 (2016).
22. Wang, X., Harris, R. E., Bayston, L. J. & Ashe, H. L. Type IV collagens regulate BMP signalling in Drosophila. *Nature* **455**, 72–77 (2008).
23. Ramírez-Weber, F. a & Kornberg, T. B. Cytonemes: cellular processes that project to the principal signaling center in Drosophila imaginal discs. *Cell* **97**, 599–607 (1999).
24. Kornberg, T. B. & Roy, S. Cytonemes as specialized signaling filopodia. *Development*

141, 729–36 (2014).

25. Van Doren, M., Williamson, A. L. & Lehmann, R. Regulation of zygotic gene expression in Drosophila primordial germ cells. *Curr Biol* **8**, 243–246 (1998).
26. McGuire, S. E., Le, P. T., Osborn, A. J., Matsumoto, K. & Davis, R. L. Spatiotemporal Rescue of Memory Dysfunction in Drosophila. *Science.* **302**, 1765–1768 (2003).
27. Roy, S., Huang, H., Liu, S. & Kornberg, T. B. Cytoneme-mediated contact-dependent transport of the Drosophila decapentaplegic signaling protein. *Science* **343**, 1244624 (2014).
28. Xie, T. & Spradling, A. C. decapentaplegic is essential for the maintenance and division of germline stem cells in the Drosophila ovary. *Cell* **94**, 251–60 (1998).
29. Inaba, M. & Yamashita, Y. M. *Evaluation of the asymmetric division of Drosophila male germline stem cells. Methods in Molecular Biology* **1463**, (2017).
30. Raj, A. & Tyagi, S. Detection of Individual Endogenous RNA Transcripts In Situ Using Multiple Singly Labeled Probes. in *Methods in enzymology* **472**, 365–386 (2010).
31. Mottier-Pavie, V. I., Palacios, V., Eliazer, S., Scoggin, S. & Buszczak, M. The Wnt pathway limits BMP signaling outside of the germline stem cell niche in Drosophila ovaries. *Dev. Biol.* **417**, 50–62 (2016).

Methods

Fly husbandry and strains. All fly stocks were raised on standard Bloomington medium at 25°C (unless temperature control was required), and young flies (0- to 4-day-old adults) were used for all experiments. The following fly stocks were used (see table1 below): tkv-YFP protein trap line (CPTI-002487) was a gift from B. McCabe. nosGal4[25], updGal4 (FBti0002638) were gift from Y. Yamashita. tubGal80^{ts} [26] (gift from C.Y. Lee), tub-GFP-Lamp1[6] (FBrf0207605, gift from H. Krämer). UAS-TIPF[11], UAS-Dpp-mCherry [27], UAS-Tkv-mCherry [27], UAS-Tkv-GFP [27] (gift from T. Kornberg and S. Roy), Oseg2 RNAi (Vienna Drosophila Resource Center, VDRC GD8122), Osm6 RNAi (VDRC GD24068), Che-13 RNAi (VDRC GD5096) and Punt-GFP (VDRC 318264, 2XTY1-SGFP-V5-preTEV-BLRP-3XFLAG). Other stocks were from Bloomington Stock Center (BDSC), UAS–GFP–αTubulin (BDSC7253); Spin RNAi (TRiP.JF02782), Lamp1 RNAi (Line1; TRiP.HMS01802 and Line2; TRiP GLV21040). For the

overexpression of Dpp-mCherry, updGal4^{ts} driver, combination of updGal4 and tubGal80^{ts} [26] was used to avoid lethality. Temperature shift crosses were performed by culturing flies at 18°C to avoid lethality during development and shifted to 29°C upon eclosion for 4 days before analysis. Control crosses for RNAi screening were designed with matching gal4 and UAS copy number using TRiP control stock (BDSC35785) at 25 ℃. RNAi screening of candidate genes for Tkv trafficking and degradation was performed by driving UAS-RNAi constructs under the control of nosGal4 or updGal4 (see below for validation method). For Dpp ts (temparature sensitive) mutant analysis, the dpphr56/CyO (BDSC36528); nos-gal4 females were crossed with dpphr4[28] (gift from Michael Buszczak) /SM6; UAS-Tkv-GFP males at permissive temperature (18 ℃) and shifted to restrictive temperature (29 ℃) upon eclosion for 24 hours before analysis.

Quantitative reverse transcription PCR.

Males carrying nos-gal4 driver were crossed with males of indicated RNAi lines or UAS–GFP–αTubulin (BDSC7253), UAS-Tkv-GFP, UASp-TkvS238A-GFP transgenic lines.

Testes from 100-200 male progenies, age 0-7 days, were collected and homogenized by pipetting in TRIzol Reagent (ThermoFisher) and RNA was extracted following the manufacturer's instructions. 1μg of total RNA was reverse transcribed to cDNA using SuperScript III First-Strand Synthesis Super Mix (ThermoFisher) with Oligo (dT)20 Primer. Quantitative PCR was performed, in duplicate, using SYBR green Applied Biosystems Gene Expression Master Mix on an CFX96 Real-Time PCR Detection System (Bio-Rad). Control primer for

αTub84B (5'-TCAGACCTCGAAATCGTAGC-3'/5'-AGCAGTAGAGCTCCCAGCAG-3')

and experimental primer for

Spin (5'-GCGAATTTCCAACCGAAAGAG-3'/5'-CGGTTGGTAGGATTGCTTCT-3')

Lamp1 (5'-AACCATATCCGCAACCATCC-3'/5'-CCTCCCTAGCCTCATAGGTAAA-3')

GFP (5'- GAACCGCATCGAGCTGAA -3'/5'-TGCTTGTCGGCCATGATATAG-3')

were used. Relative quantification was performed using the comparative CT method (ABI manual). (Lamp1 Line1; TRiP.HMS01802 47.79%, Line2; TRiP GLV21040 50.87%, Spin 25.05%). Other RNAi lines were validated previously[5]. GFP mRNA levels of nos>Tkv-GFP and in nos>TkvS238A were 84.6% and 74.2% of nos>UAS–GFP–αTubulin expression level respectively.

Generation of Tkv S238A transgenic flies. EGFP cDNA were amplified from Drosophila gateway pPGW vector (https://emb.carnegiescience.edu/drosophila-gateway-vector-collection#_Copyright,_Carnegie) using following primers with restriction sites (underlined).

BglII GFP F 5'- ACAGATCTATGGTGAGCAAGGGCGAGGAGCTGTTCA-3'

AscI GFP R 5'-TAGGCGCGCCTTACTTGTACAGCTCGTCCATGCCGAGA-3'

then digested with BglII and AscI. NotI BglII sites (underlined) were attached to gBlock TkvS238A fragment (Integrated DNA Technologies, sequence as follows).

5'-

ATGCGGCCGCACCATGGCGCCGAAATCCAGAAAGAAGAAGGCTCATGCCCGCTCCCTAACC
TGCTACTGCGATGGCAGTTGTCCGGACAATGTAAGCAATGGAACCTGCGAGACCAGACCCG
GTGGCAGTTGCTTCAGCGCAGTCCAACAGCTTTACGATGAGACGACCGGGATGTACGAGGA
GGAGCGTACATATGGATGCATGCCTCCCGAAGACAACGGTGGTTTTCTCATGTGCAAGGTAG
CCGCTGTACCCCACCTGCATGGCAAGAACATTGTCTGCTGCGACAAGGAGGACTTCTGCAAC
CGTGACCTGTACCCCACCTACACACCCAAGCTGACCACACCAGCGCCGGATTTGCCCGTGAG
CAGCGAGTCCCTACACACGCTGGCCGTCTTTGGCTCCATCATCATCTCCCTGTCCGTGTTTAT
GCTGATCGTGGCTAGCTTATGTTTCACCTACAAGCGACGCGAGAAGCTGCGCAAGCAGCCAC
GTCTCATCAACTCAATGTGCAACTCACAGCTGTCGCCTTTGTCACAACTGGTGGAACAGAGT
TCGGGCGCCGGATCGGGATTACCATTGCTGGTGCAAAGAACCATTGCCAAGCAGATTCAGAT
GGTGCGACTGGTGGGCAAAGGACGATATGGCGAGGTCTGGCTGGCCAAATGGCGCGATGAG
CGGGTGGCCGTCAAGACCTTCTTTACGACCGAAGAGGCTTCTTGGTTCCGCGAGACTGAAAT
CTATCAGACAGTGCTGATGCGACACGACAATATCTTGGGCTTCATTGCCGCCGATATCAAGG
GTAATGGTAGCTGGACACAGATGTTGCTGATCACCGACTACCACGAGATGGGCAGCCTACA
CGATTACCTCTCAATGTCGGTGATCAATCCGCAGAAGCTGCAATTGCTGGCGTTTTCGCTGG
CCTCCGGATTGGCCCACCTGCACGACGAGATTTTCGGAACCCCTGGCAAACCAGCTATCGCT
CATCGCGATATCAAGAGCAAGAACATTTTGGTCAAGCGGAATGGGCAGTGCGCTATTGCTG
ACTTCGGGCTGGCAGTGAAGTACAACTCGGAACTGGATGTCATTCACATTGCACAGAATCCA
CGTGTCGGCACTCGACGCTACATGGCTCCAGAAGTATTGAGTCAGCAGCTGGATCCCAAGCA
GTTTGAAGAGTTCAAACGGGCTGATATGTATTCAGTGGGTCTCGTTCTGTGGGAGATGACCC
GTCGCTGCTACACACCCGTATCGGGCACCAAGACGACCACCTGCGAGGACTACGCCCTGCCC
TATCACGATGTGGTGCCCTCGGATCCCACGTTCGAGGACATGCACGCTGTTGTGTGCGTAAA
GGGTTTCCGGCCGCCGATACCATCACGCTGGCAGGAGGATGATGTACTCGCCACCGTATCCA
AGATCATGCAGGAGTGCTGGCACCCGAATCCCACCGTTCGGCTGACTGCCCTGCGCGTAAAG
AAGACGCTGGGGCGACTGGAAACAGACTGTCTAATCGATGTGCCCATTAAGATTGTCAGATC
TCA-3'

Synthesized fragments were annealed and digested by NotI and BglII. Resultant two inserts (TkvS238A and GFP) were ligated to modified pPGW vector using NotI and AscI sites in the multiple cloning site. Transgenic flies were generated using strain attP2 by PhiC31 integrase-mediated transgenesis (BestGene Inc.).

Generation of nos-loxP-mCherry-loxP-gal4-VP16 transgenic flies.

Step1: Construction of loxP-mCherry-SV40-loxP. mCherry cDNA was amplified using primers NheI mCherry Fw (5'-acgctagctatggtgagcaagggcgaggag-3') and XhoI mCherry Rv (5'-gactcgagttacttgtacagctcgtccat-3') from mCherry Vector (Clontech), and then the product was introduced into NheI-XhoI sites of the pFRT-SV40-FRT vector (Gift from Elizabeth R. Gavis). Step2: BamHI-loxP-NotI oligo (5'-GATCCATAACTTCGTATAGCATACATTATACGAAGTTATGC-3', 5'-GGCCGCATAACTTCGTATAATGTATGCTATACGAAGTTATG-3') was inserted into BamHI NotI site after the SV40 polyA sequence of StepI vector. NdeI-loxP-NheI oligo (5'-CATATGCAACATGATAACTTCGTATAGCATACATTATACGAAGTTATTG-3', 5'-CTAGCAATAACTTCGTATAATGTATGCTATACGAAGTTATCATGTTGCATATGCATG- 3') was inserted into NdeI/NheI site upstream of mCherry sequence of Step1 vector. Step3: The NotI-BamHI flanked 3.13-Kb fragment from the pCSpnosFGVP (Gift from Elizabeth R. Gavis) containing the Nanos 5' region-ATG (NdeI-start codon) Gal4-VP16-Nanos 3' region was subcloned into NotI-BamHI sites of pUAST-attB. Step4: The NdeI-flanked loxP-mCherry-SV40 polyA-loxP fragment was subcloned into the NdeI start codon of the plasmid described in Step3. A transgene was introduced into the attP2 using PhiC31 integrase-mediated transgenesis systems by BestGene, Inc.

Immunofluorescent Staining. Immunofluorescent staining was performed as described previously[29]. Briefly, testes were dissected in phosphate-buffered saline (PBS) and fixed in 4% formaldehyde in PBS for 30–60 minutes. Next, testes were washed in PBST (PBS +0.3% TritonX-100) for at least 30 minutes, followed by incubation with primary antibody in 3% bovine serum albumin (BSA) in PBST at 4 °C overnight. Samples were washed for 60 minutes (three times for 20minutes each) in PBST, incubated with secondary antibody in 3% BSA in PBST at 4 °C overnight, and then washed for 60 minutes (three times for 20 minutes each) in PBST. Samples were then mounted using VECTASHIELD with 4′,6-diamidino-2-phenylindole (DAPI) (Vector Lab, H-1200).

The primary antibodies used were as follows: 1B1 and rat anti Vasa (1:20), obtained from the Developmental Studies Hybridoma Bank (DSHB), Rabbit anti-Smad3 (phospho S423 + S425) antibody (1:100, Abcam, ab52903) AlexaFluor-conjugated secondary antibodies were used at a dilution of 1:400. Images were taken using a Zeiss LSM800 confocal microscope with a 63 ×oil immersion objective (NA=1.4) and processed using Image J and Adobe Photoshop software. Three-dimensional rendering was performed by Imaris software.

In situ hybridization

In situ hybridization on adult testes was performed as described previously[30].
Briefly, testes were dissected in 1XPBS and then fixed in 4% formaldehyde/PBS for 45 min. After rinsed 2 times with 1XPBS, then resuspended in 70% EtOH, left overnight at 4°C. The next day, testes were washed briefly in the wash buffer containing 2XSSC and 10% deionized formamide, then incubated overnight at 37°C in the dark with the 50nM of Quasar® 570 labeled stellaris probe against dpp mRNA (LGC Biosearch Technologies, kind gift from Michael Buszczak, previously validated[31]) in the Hybridization Buffer containing 2XSSC, 10% Dextran sulfate (MilliporeSigma), 1μg/μl of yeast tRNA (MilliporeSigma), 2mM Vanadyl ribonucleoside complex (NEB), 0.02% RNAse free BSA (ThermoFisher) and 10% of deionized formamide. On the 3rd day, testes were washed 2 times for 30 min each at 37°C in the dark in the prewarmed wash buffer and then resuspended in a drop of VECTASHIELD with DAPI (Vector Lab, H-1200).

Chloroquine or Lysotracker/LysoSensor treatment

Testes from newly eclosed flies were dissected into Schneider's Drosophila medium containing 10% fetal bovine serum. Then testes were incubated at room temperature with or without 100μM Chloroquine (Sigma) in 1mL media for 4 hours or 2 hours prior to imaging. For the lysosome staining, testes were incubated with 50nM of LysoTracker Deep Red (ThermoFisher L12492) or 100nM of LysoSensor Green DND-189 (ThermoFisher L7535) probes in 1mL media for 10 min at room temperature then briefly rinsed with 1mL of media for 3 times prior to imaging. For Tkv-mCherry clonal expression, hs-cre, nos-loxP-stop-loxP-Gal4 with UAS-Tkv-mCherry, UAS-GFP-αTubulin flies were heat-shocked at 37°C. for 15 min. Testes were dissected 24 hour-after the heat shock.
These testes were placed onto Gold Seal™ Rite-On™ Micro Slides two etched rings with media, then covered with coverslips. An inverted Zeiss LSM800 confocal microscope with a 63 ×oil immersion objective (NA=1.4) was used for imaging.
For the Chloroquine feeding, newly eclosed flies were starved for overnight then transferred to food containing 3 mg/ml chloroquine (Sigma) for 3 days.

Quantification of pMad intensities.

Integrated intensity within the GSC nuclear region was measured for anti-pMad staining and divided by the area. To normalize the staining condition, data were further normalized by the average intensities of pMad from randomly picked three cyst cells in the same testes, and the ratios of relative intensities were calculated as each GSC per average cyst cell.

Quantification of Dpp (Dpp-mCherry or Dpp-GFP) intensities.

From a single stack at the level of hub centre, 3 randomly selected squares (5μmX5μm) within 10μm wide region outside of the hub (located next to the hub edge) were measured and background levels were subtracted and normalized by divisions by the mean intensity from 3 randomly selected lysosomal Dpp signal in the same image. Note; Although lysosomal Dpp signal increases size and number in the hub after CQ treatment, but intensity/area did not change.

FRAP analysis.

Fluorescence recovery after photo-bleaching (FRAP) of Dpp-mCherry signal was undertaken using a Zeiss LSM800 confocal laser scanning microscope with 63X/1.4 NA oil objective. Zen black software was used for programming of each experiment. A small region (<10μm diameter) of interest was photobleached using laser powers to achieve an approximately 50%-70% bleach using the combination of 405, 480, 555, 640 nm laser. Fluorescence recovery was monitored every second for up to 10 minutes.

Statistical analysis and graphing.

No statistical methods were used to predetermine sample size. The experiments were not randomized. The investigators were not blinded to allocation during experiments and outcome assessment.

Statistical analysis and graphing were performed using Microsoft Excel 2010 or GraphPad prism 7 software. Data are means and standard deviations.

The P values (two-tailed Student's t-test or adjusted *P* values from Dunnett's multiple comparisons test) are provided and shown as *P<0.05, **P<0.01, ***P<0.001, ****P<0.0001; or non-significant if not shown (P>0.05).

Figure 1

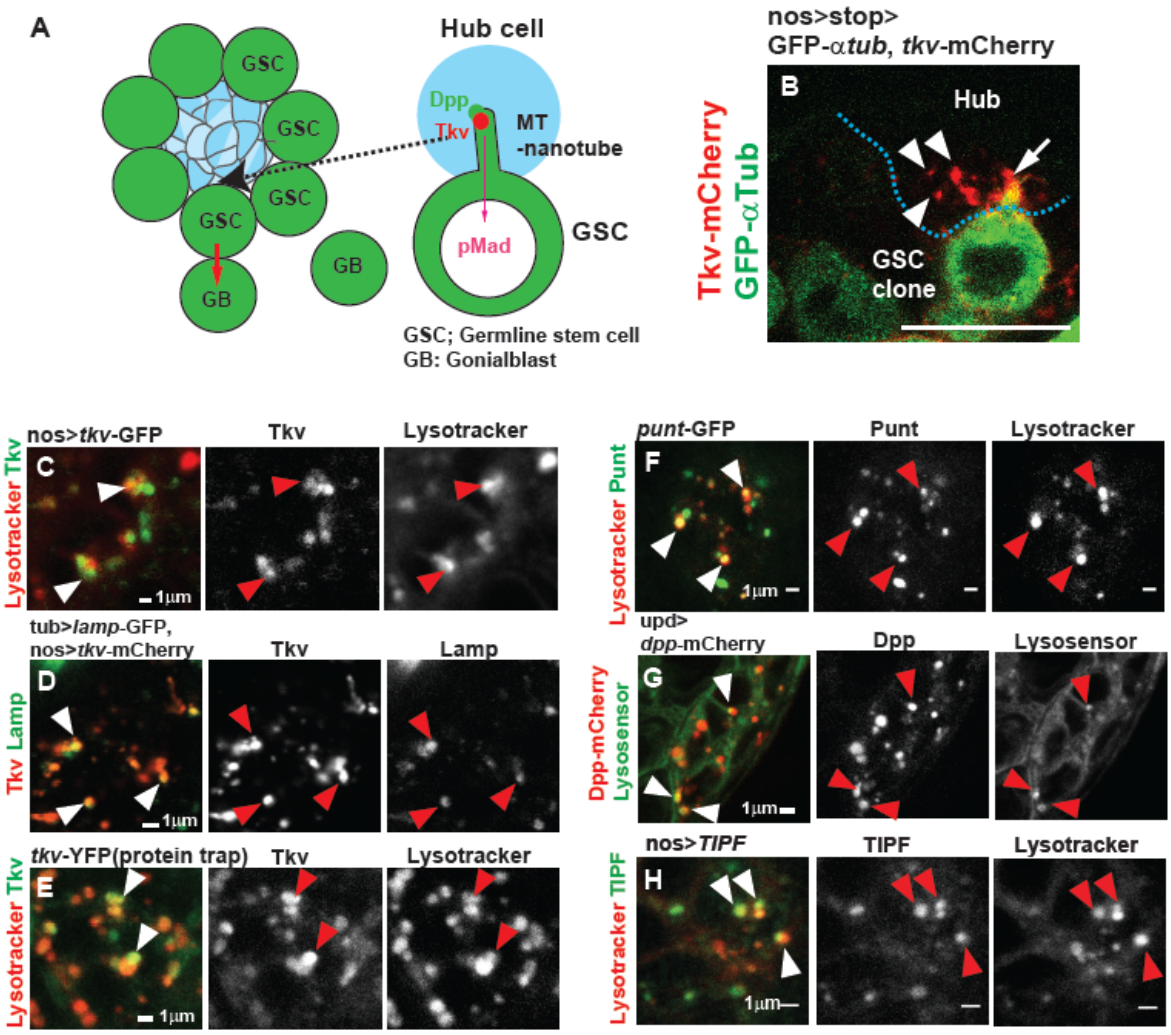
A
Hub cell
GSC
GSC
GSC
GSC
GB
GB
Dpp
Tkv
MT
-nanotube
pMad
GSC
GSC; Germline stem cell
GB: Gonialblast
nos>stop>
GFP-αtub, tkv-mCherry
B
Hub
GSC
clone
Tkv-mCherry
GFP-αTub
nos>tkv-GFP
Tkv
Lysotracker
C
Lysotracker Tkv
1μm
tub>lamp-GFP,
nos>tkv-mCherry
Tkv
Lamp
D
Tkv Lamp
1μm
tkv-YFP(protein trap)
Tkv
Lysotracker
E
Lysotracker Tkv
1μm
punt-GFP
Punt
Lysotracker
F
Lysotracker Punt
1μm
upd>
dpp-mCherry
Dpp
Lysosensor
G
Dpp-mCherry
Lysosensor
1μm
nos>TIPF
TIPF
Lysotracker
H
Lysotracker TIPF
1μm

Figure 2

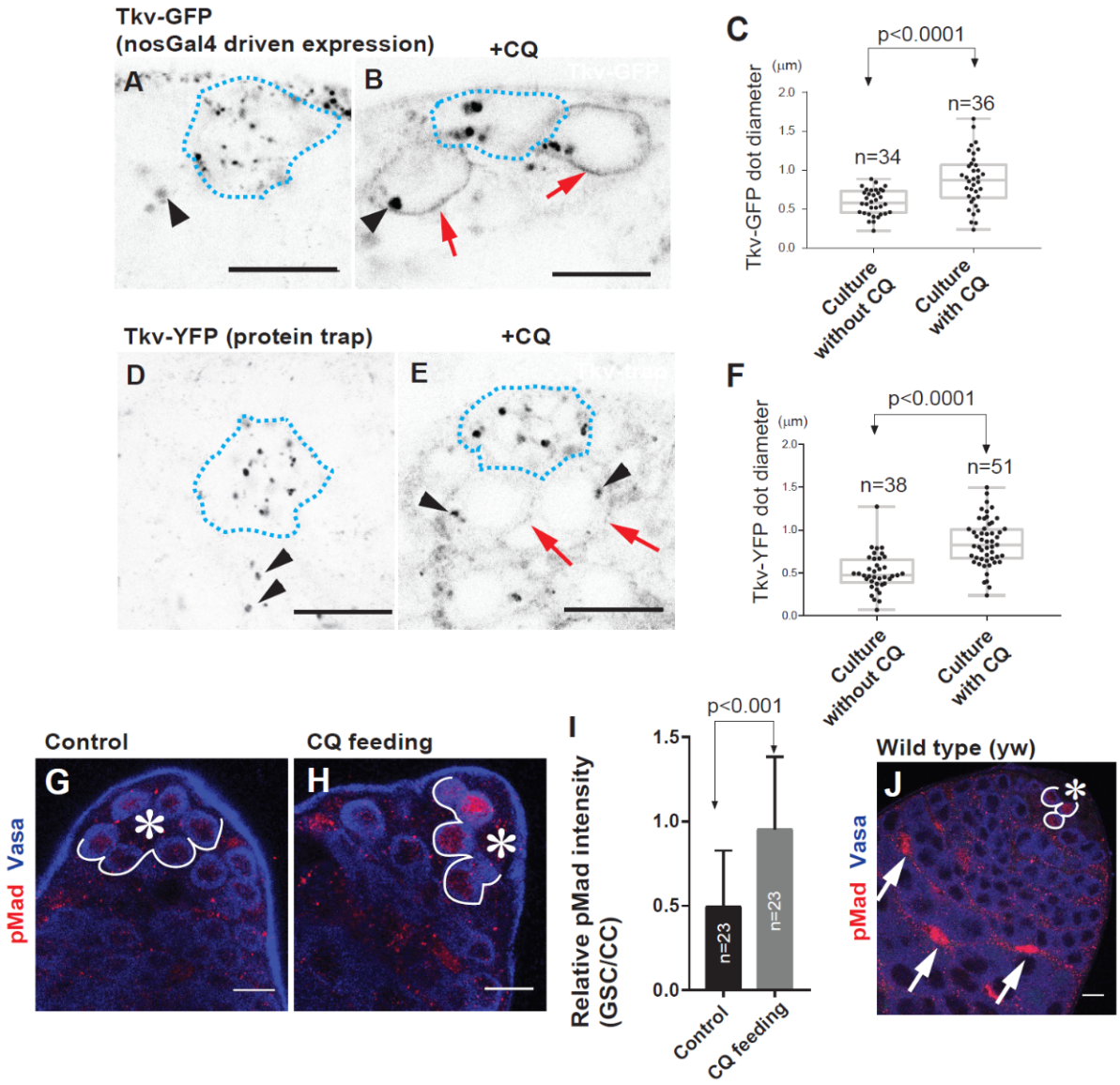
Tkv-GFP
(nosGal4 driven expression)
+CQ
A
B
C
p<0.0001
(μm)
Tkv-GFP dot diameter
n=34
n=36
Culture without CQ
Culture with CQ
Tkv-YFP (protein trap)
+CQ
D
E
F
p<0.0001
Tkv-YFP dot diameter
n=38
n=51
Culture without CQ
Culture with CQ
Control
CQ feeding
G
H
pMad Vasa
I
p<0.001
Relative pMad intensity (GSC/CC)
n=23
n=23
Control
CQ feeding
Wild type (yw)
J
pMad Vasa

Figure 3

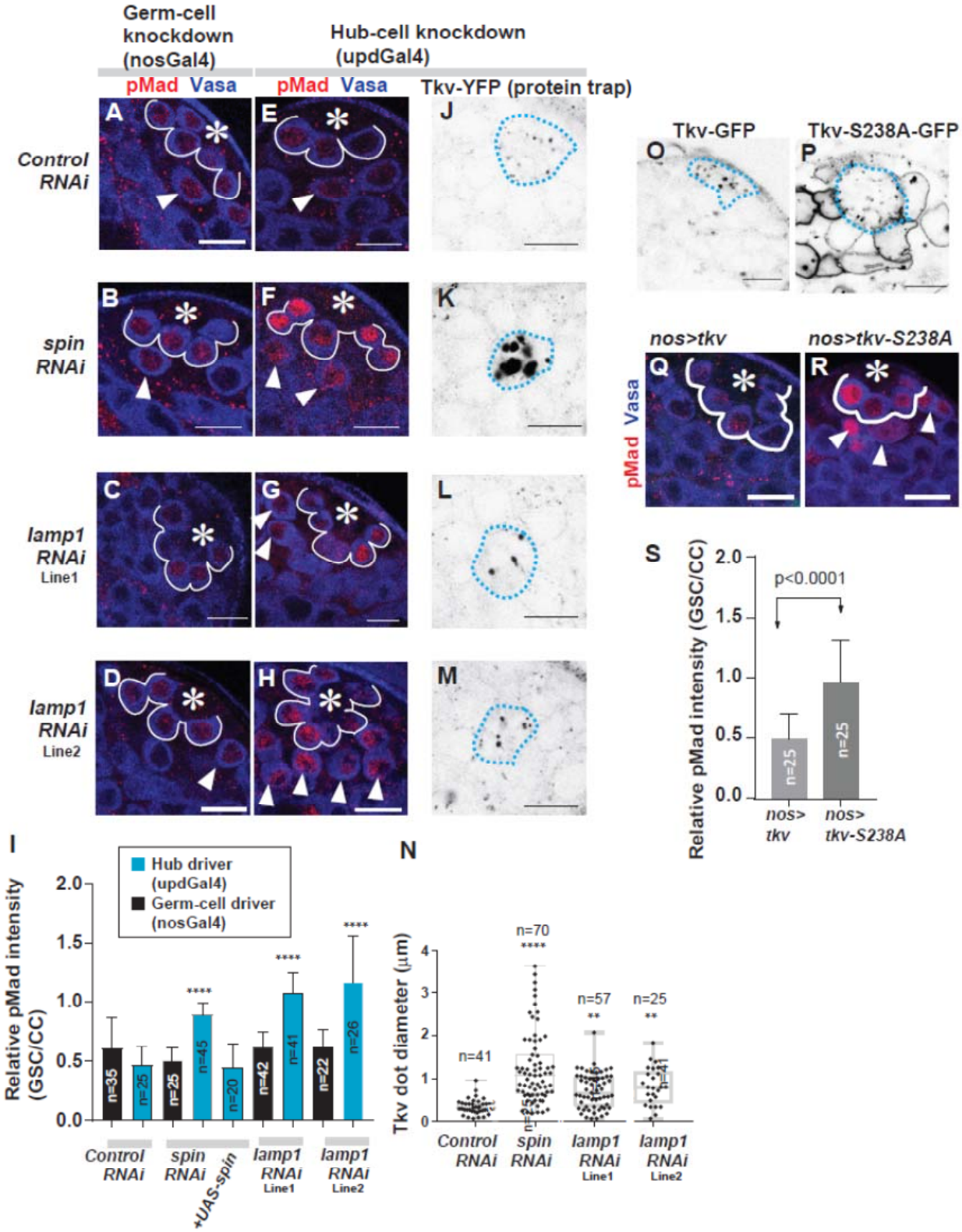
Germ-cell knockdown (nosGal4)
Hub-cell knockdown (updGal4)
pMad Vasa
pMad Vasa
Tkv-YFP (protein trap)
Control RNAi
spin RNAi
lamp1 RNAi Line1
lamp1 RNAi Line2
Tkv-GFP
Tkv-S238A-GFP
nos>tkv
nos>tkv-S238A
pMad Vasa
Relative pMad intensity (GSC/CC)
p<0.0001
nos> tkv
nos> tkv-S238A
Hub driver (updGal4)
Germ-cell driver (nosGal4)
Control RNAi
spin RNAi
+UAS-spin
lamp1 RNAi Line1
lamp1 RNAi Line2
Tkv dot diameter (µm)

Figure 4

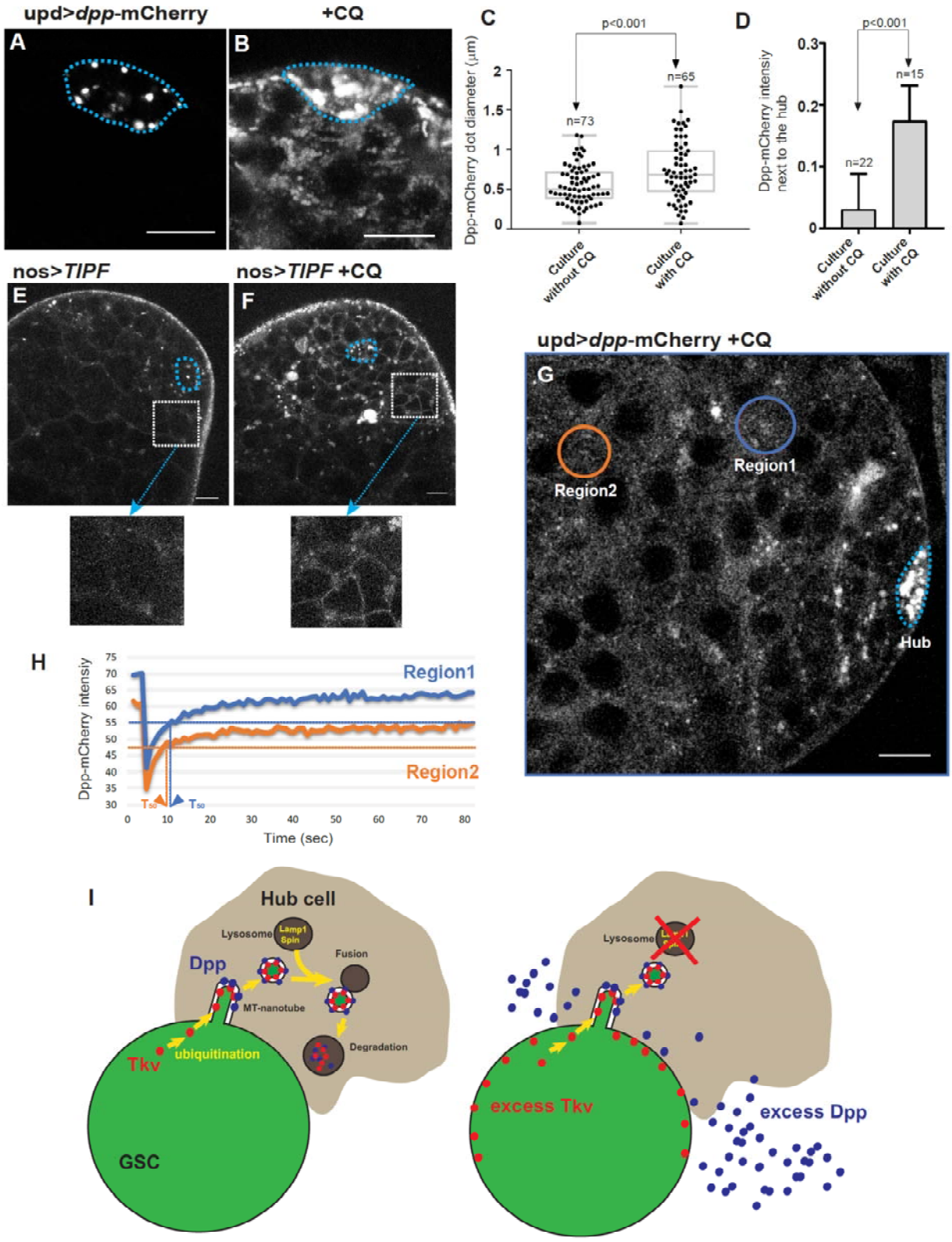
upd>dpp-mCherry
+CQ
A
B
C
p<0.001
n=73
n=65
Dpp-mCherry dot diameter (μm)
Culture without CQ
Culture with CQ
D
p<0.001
n=22
n=15
Dpp-mCherry intensiy next to the hub
nos>TIPF
nos>TIPF +CQ
E
F
upd>dpp-mCherry +CQ
G
Region1
Region2
Hub
H
Dpp-mCherry intensiy
Region1
Region2
Time (sec)
I
Hub cell
Lysosome
Lamp1 8pin
Fusion
Dpp
MT-nanotube
Degradation
Tkv
ubiquitination
GSC
excess Tkv
excess Dpp

Figure legends

Figure 1. Tkv receptor that is expressed in GSCs, localizes to hub cell lysosomes. A, left, Schematic of the *Drosophila* male GSC niche. GSCs are attached to the hub. The immediate daughters of GSCs, the gonialblasts (GBs) are displaced away from the hub then start differentiation. A mitotic GSC is shown carrying a spindle that is perpendicular to the hub-GSC interface, leading to division orientation (red arrow indicates the division orientation of the daughter cells). **Right,** MT-nanotube-mediated Dpp ligand-Tkv receptor interaction at the hub cell-GSC boundary. **B,** A GSC clone expressing Tkv-mCherry (red), GFP-αTub (green). Arrow indicates a MT-nanotube illuminated by GFP-αTub and Tkv-mCherry. Arrowheads indicate localization of Tkv-mCherry outside of the MT-nanotube within hub cells. **C-H,** Representative images of hub area. **C,** Tkv-GFP expressed under the germline specific driver (nosGal4) colocalizing with the lysotracker positive lysosomes in the hub. **D,** Tkv-mCherry expressed in germline colocalizing with *lamp*-GFP positive lysosomes in the hub. **E**, Protein trap lines for Tkv (*tkv-*YFP). **F,** TypeII receptor Punt (*punt*-GFP) localizing in the hub lysosomes (Lysotracker). **G,** Dpp-mCherry expressed under the hub specific driver (updGal4^{ts}) localizing in the hub lysosomes (lysosensor). **H,** TIPF expressed under the germline specific driver (nosGal4). localizing in the hub lysosomes (Lysotracker). **C-H,** Arrowheads indicate colocalization (yellow) of green and red from each genotype. Scale bars, 10μm in **B**, 1μm in **C-H**.

Figure 2. Chloroquine suppresses Tkv degradation in hub cells and downstream signal activation in GSCs

A, B Representative images of the hub area surrounded by Tkv-GFP-expressing GSCs in 4-hour cultured testes without (**A**) or with (**B**) chloroquine (+CQ). The hub is encircled by a blue dotted line. In the presence of CQ, Tkv-GFP punctae are larger. Red arrows indicate GSCs with cell body (plasma membrane) localization of Tkv. Black arrowheads indicate Tkv punctae within GSCs. **C,** Measured diameters of Tkv punctae in the hub with or without CQ (largest diameter chosen from 0.5 μm interval z-stacks for each dot). Indicated numbers of punctate from two independent experiments were scored for each data point. **D-F,** Results similar to those shown in **A-C**, using a tkv-YFP protein trap line. **G, H,** Representative images of the testes after 4-hour incubation in the media without (CQ-

) or with (CQ+) Chloroquine. **I,** Quantitation of pMad intensity in the GSCs (relative to somatic cyst cells; CCs, see **J** and method). Indicated numbers of GSCs from two independent experiments were scored for each data point. **J,** A representative image of pMad labelling (red) in the wild type (yw: yellow white) testis. Red arrows indicate the pMad signal in CCs which were used as an internal control for pMad staining. **G-J** White lines divide GSCs attached to the hub and their immediate progeny.

Scale bars, 10μm. Asterisks indicate the hub. The *P* values were calculated by a student t-test P values.

Figure 3. Hub lysosomes are responsible for Dpp signal suppression.

A-H, Representative images of pMad staining (red) in testis of the indicated genotypes. Drivers specific for the germline (nosGal4) or hub cells (updGal4) used to cause expression of the indicated RNAi. Asterisks indicate the hub. White lines divide GSCs attached to the hub and their immediate progeny. Arrowheads indicate cells away from the hub which remain pMad positive, more frequently seen in **F, G, H** than control (**E**) or nosGal4 mediated knock down (**A-D**). Vasa (blue); germ cell marker. **I,** Quantitation of pMad intensity in the GSCs (relative to CC, see methods and Figure 2J). Indicated numbers of GSCs from two independent experiments were scored for each data point.

J-M, Representative images of Tkv-trap punctae in the hub (encircled by blue dotted lines) with hub cell specific RNAi of indicated genes. **N,** Measured diameters of Tkv-YFP punctae in the hub from indicated genotypes (largest diameter chosen from 0.5 μm interval z-stacks for each dot). The indicated numbers (n) of dots from two independent experiments were scored for each data point. Scale bars, 10 μm. Data are means and standard deviations. P values (**P<0.01, ****P<0.0001) are shown. Adjusted *P* values were calculated by Dunnett's multiple comparisons.

O, P, Representative images of the testis tips with nosGal4 mediated expression of tkv-GFP or tkvS238A-GFP (**O,** nosGal4>*tkv*-GFP, **P,** nosGal4>*tkv*S238A-GFP) **Q, R,** Representative images of pMad staining in the testes with Tkv-GFP expression (**Q**), or TkvS238A-GFP expression (**R**), White lines divide GSCs attached to the hub and their immediate progenies. Arrowheads indicate cells away from the hub which remain pMad (red) positive. Vasa (blue); germ cell marker. **S,** Quantitation of pMad intensity in the GSCs (relative to CC) of Tkv- or TkvS238A-expressing testes. The indicated numbers of GSCs from two independent experiments were scored for each data point. Scale bars, 10 μm unless otherwise stated. Data are means and standard deviations. *P* values were calculated by student-t-tests.

Figure 4. Lysosomal inhibition visualizes Dpp diffusion

A, B, Representative images of the testis tips with expression of Dpp-mCherry under the control of a hub specific driver (updGal4>*dpp*-mCherry) after 2-hour culture without (**A**) or with (**B**) CQ. **C,** Diameters of Dpp punctae in the hub after incubation with or without CQ. For the measurement, only well isolated dot was picked to avoid measuring overlapped 2 or more lysosomes. To select single, well-separated lysosomes, lower laser exposure was used. **D,** Average intensities of Dpp-mCherry signal in randomly selected 5μmX5μm square areas next to the hub (see method for measurement). In **C,** largest diameter chosen from 0.5 μm interval z-stacks for each dot. The indicated numbers (n) of dots from two independent experiments were scored for each data point. Box plot shows 25–75% (box), median (band inside) and minima to maxima (whiskers). The indicated numbers (n) of testes from two independent experiments were scored for each data point.
E, F, Representative images of the testis tips with expression of Tkv activation sensor, TIPF, under the control of a germline specific driver (nosGal4>TIPF) after 4-hour culture without (**E**) or with (**F**) CQ. Insets show magnified images from squared regions.
G, Representative FRAP experiments of the testis tips with expression of Dpp-mCherry after 2-hour chloroquine treatment. Two regions were photobleached and monitored the recovery indicated time points. **H,** Measured intensities (-BG; background subtracted) of the Dpp-mCherry signal from each region. Both regions show rapid recovery after bleaching. Lines indicate 50% intensity of initial levels. Arrowheads (T50) indicate the timepoints at which 50% of the original intensity was reashced. **I,** Model. **Left;** Tkv expressed in GSC is transferred to hub lysosomes through MT-nanotubes, where Tkv is subjected to lysosomal degradation. This way, MT-nanotubes contribute to both signal activation and inactivation. **Right;** Hub lysosomal inhibition initiates excess Tkv retention within GSC and excess Dpp ligand start diffusing out from the niche.

The *P* value was calculated by a student t-test. Scale bars, 10mm. The hub is encircled by blue dotted line.

Figure S1

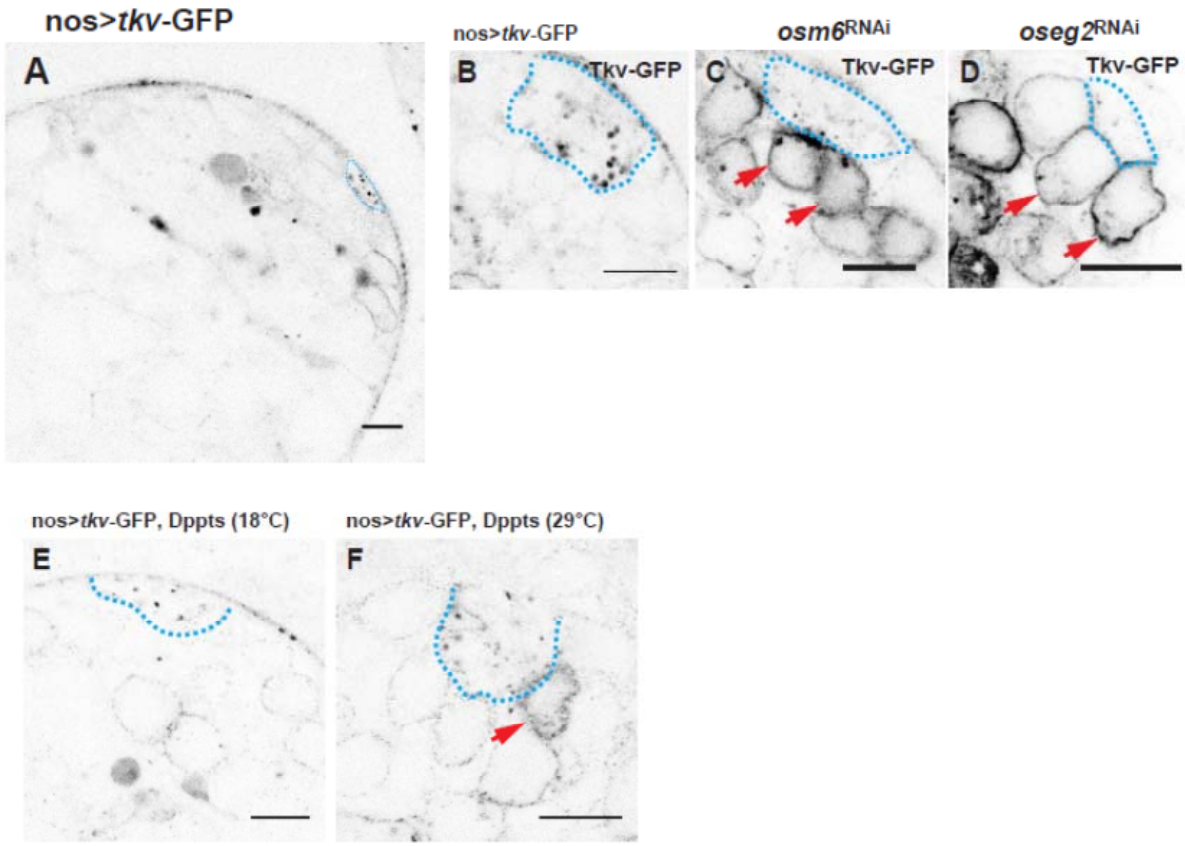

A, Tkv-GFP localization in the testis. Tkv signal is limited in hub (A). B) Tkv localization to the hub or GSC plasma membrane in control (B) and knock down of three IFT-B (Intraflagellar transport-B) genes, *osm6* RNAi (C) and *oseg2* RNAi (D), Dpp ts mutant background in permissive (18°C) temperature (E) or restrictive (29°C) temperature (F). Dotted blue line indicates the hub. Arrows indicate plasma membrane localization of Tkv. Scale bars, 10 µm.

Figure S2

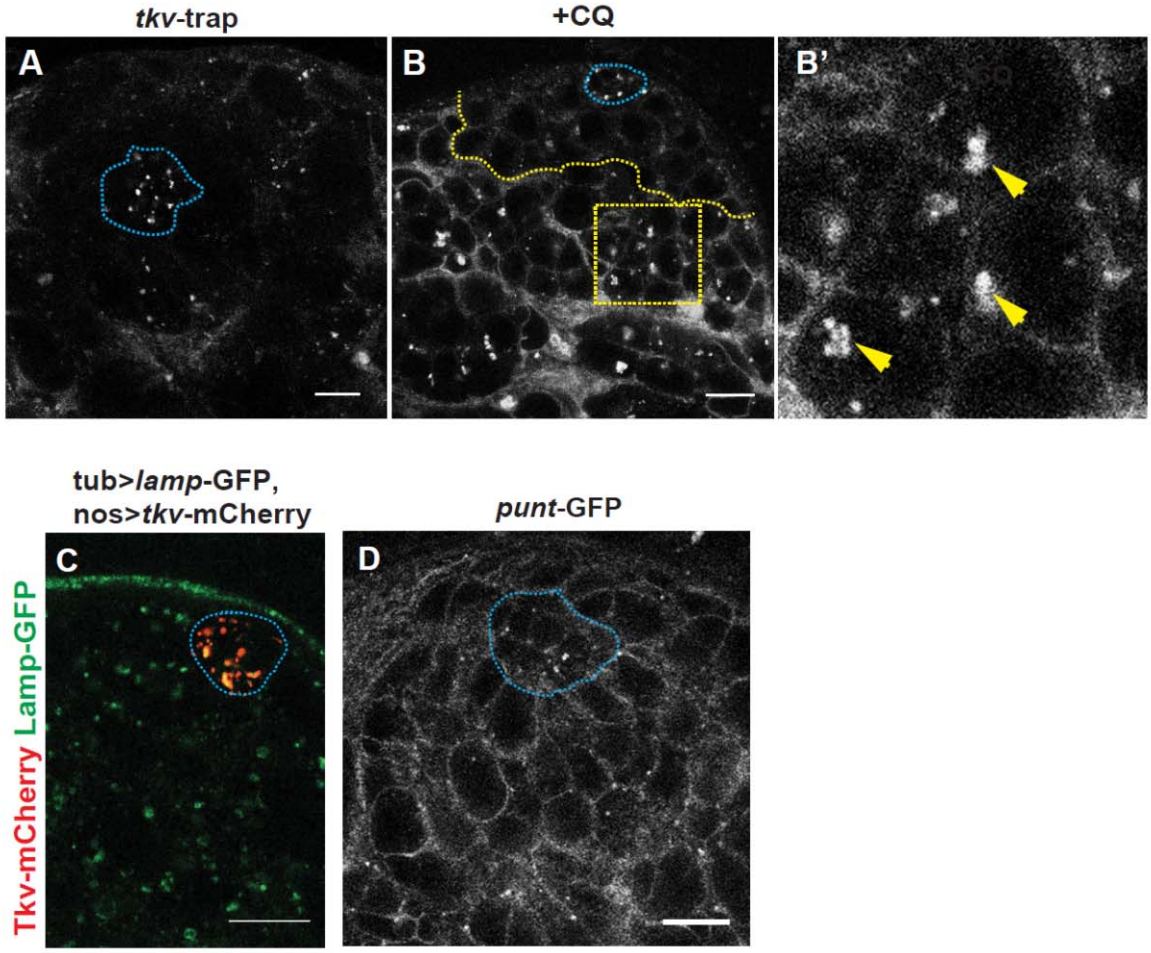

A, Tkv protein trap localization in the testis. Tkv signal is limited in hub. **B, B',** Localization of Tkv protein trap in the testis after Chloroquine treatment. Tkv localized to enlarged lysosomes in the hub. Tkv-trap signal in the lysosome and plasma membrane of later stage spermatogonia (Figure S2B, distal from yellow broken line, and B' yellow arrowheads), indicating that spermatogonia likely utilize their own lysosomes to degrade Tkv. **C,** tubGal4-driven-lamp-GFP localization in the testis (green). nosGal4-driven-tkv-mCherry localizes to hub often colocalizing with Lamp-GFP dots. **D,** TypeII receptor Punt-GFP localization in the testis. Dotted blue line indicates the hub. Arrows indicate plasma membrane localization of Tkv. Scale bars, 10 μm.

Figure S3

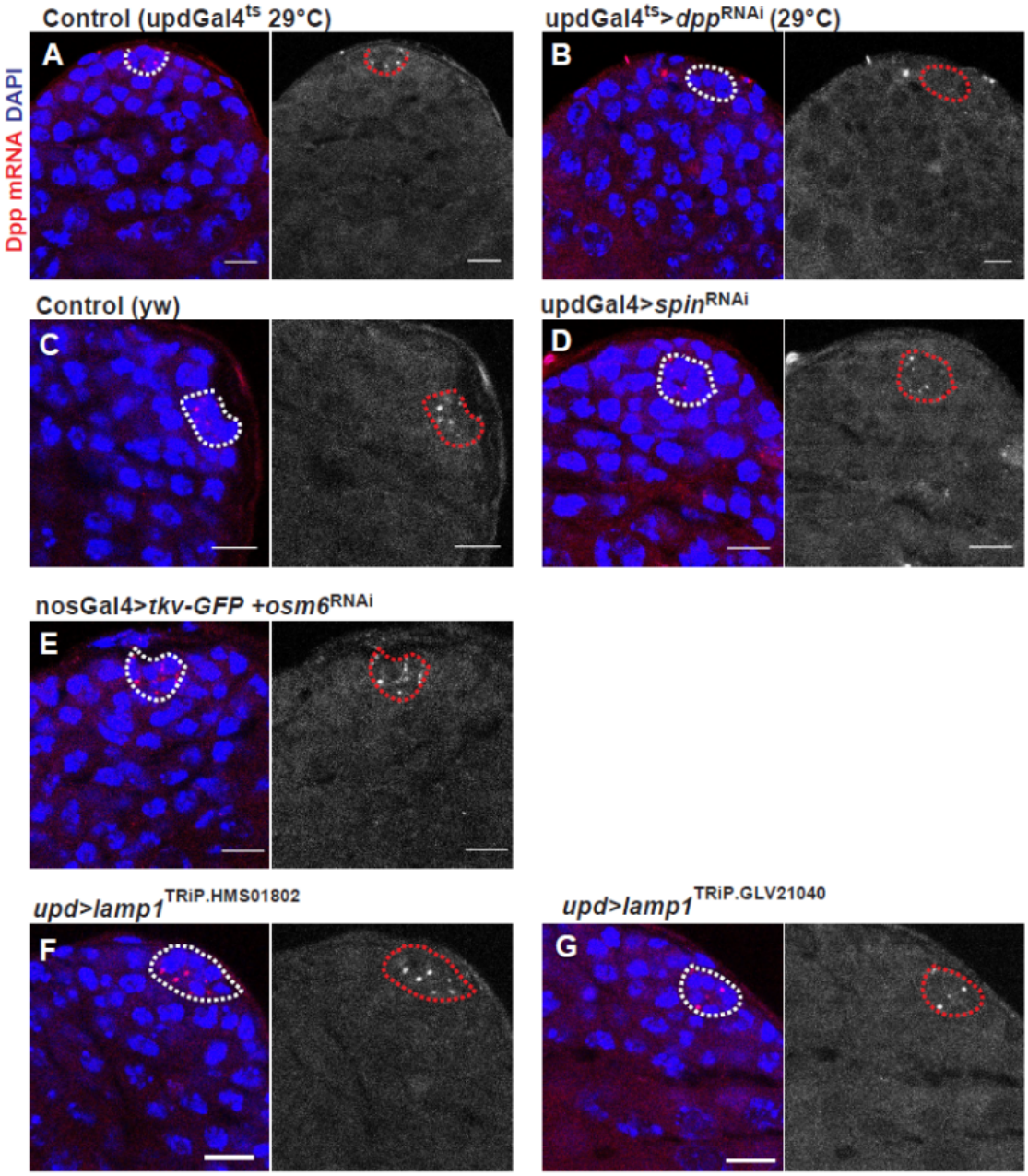

A-G, Representative images of *in situ* hybridization using Stellaris FISH probe against *dpp* mRNA (red) in the testis of indicated genotypes. **B,** Dpp RNAi (negative control) testis shows almost no detectable signal in the hub, suggesting the specificity of the probe. Hub is encircled by a white dotted line. DAPI (blue). Scale bars, 10 µm.

Figure S4

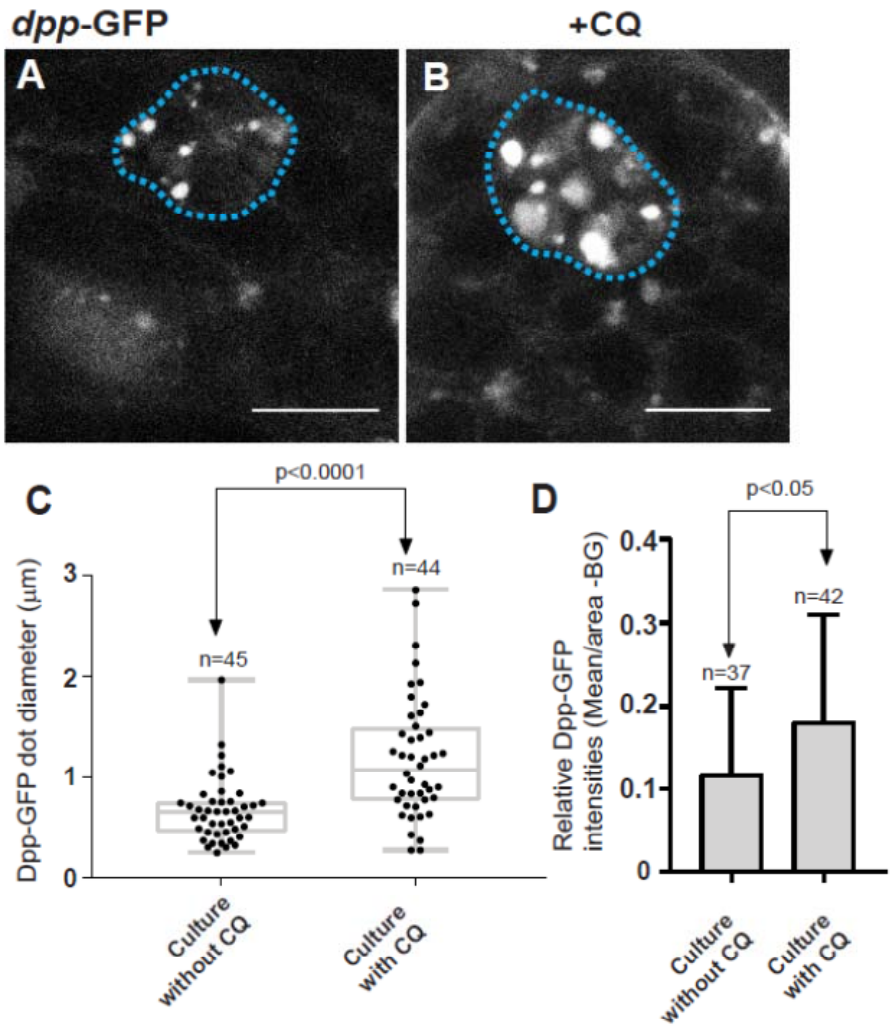

A, B Representative images of the testis tips from flies with Dpp-GFP fosmid genomic construct under the after 2-hour culture without (**E**) or with (**F**) CQ. **C,** Diameters of Dpp punctae in the hub after incubation with or without CQ. For the measurement, only well isolated dot was picked to avoid measuring overlapped 2 or more lysosomes. To select single, well-separated lysosomes, lower laser exposure was used. **D,** Average intensities of Dpp-GFP signal in randomly selected 5µmX5µm square areas next to the hub (see method for measurement). In **C,** largest diameter chosen from 0.5 µm interval z-stacks for each dot. The indicated numbers (n) of dots from two independent experiments were scored for each data point. Box plot shows 25–75% (box), median (band inside) and minima to maxima (whiskers). The indicated numbers (n) of testes from two independent experiments were scored for each data point. The indicated numbers (n) of testes from two independent experiments were scored for each data point. The *P* value was calculated by a student t-test. Scale bars, 10mm. The hub is encircled by blue dotted line.

Supplementary videos

Movie1; A representative movie of Dpp-mCherry expressed in the hub. Images were taken every second for 30 seconds.
Movie2; A representative movie of Dpp-mCherry diffusion after chloroquine treatment (see Figure5A). Images were taken every second for 26 secounds.

Movie 3; Quick recovery of the signal after photo bleaching (Figure5D Region1). Images were taken every second for 20 seconds.
Movie 4; Quick recovery of the signal after photo bleaching (Figure5D Region2). Images were taken every second for 20 seconds.

Movie 5; A representative video of Dpp-mCherry punctum (Lysosome) within hub cell after photo bleaching. Images were taken every 5 seconds for 35 secounds.

Table1

Genotype	Tkv localization/distribution
nosGal4>Tkv-GFP	Punctae in the hub
Tkv-YFP protein trap	Punctae in the hub
nosGal4>Tkv-S238A-GFP	GSC cell body (entire plasma membrane)
nosGal4>Tkv-GFP +CQ	Larger punctae in the hub, GSC cell body
Tkv-YFP protein trap +CQ	Larger punctae in the hub, GSC cell body (weak signal)
nosGal4>Tkv-GFP+IFT-B (Osm6, Oseg2 or Che-13) RNAi	GSC cell body (entire plasma membrane)
updGal4>Lamp RNAi Line1 and Line2 Tkv-YFP protein trap	Larger punctae in the hub, GSC cell body (weak signal)
updGal4>Spin RNAi Tkv-YFP protein trap	Larger punctae in the hub, GSC cell body (weak signal)
Dpp ts mutant (TS Day3) Tkv-YFP protein trap	GSC cell body (weak signal)

Tkv localization/distribution pattern after inhibition of hub degradation using indicated treatment/genotypes.

Table2

Genotype	Stock information	Purpose	References
nosGal4 VP16		Germline specific expression of Gal4	[25]
updGal4	FBti0002638	Hub specific expression of Gal4	
updGal4ts		Hub specific expression of Gal4 released from tubGal80ts surpression at permissive temparature (29°C)	[26]
hs-cre, nos-loxP-stop-loxP-Gal4	this study	Start Gal4 expression (no GFP) in germline after Stop codon is removed by heat-shock mediated Cre recombination	
UASp-TkvS238A-GFP	this study	Tkv-S238A mutant form GFP fusion expressing under UAS promoter	
tkv-YFP protein trap	CPTI-002487	YFP (Yellow fluorescent protein) is inserted within 5' of endogenous Tkv locus making N terminus fusion with endogenous Tkv protein	
Oseg2 RNAi	VDRC GD8122	hairpin RNA against Oseg2 gene expressing under UAS promoter	
Che-13 RNAi	VDRC GD5096	hairpin RNA against Che-13 gene expressing under UAS promoter	
Osm6 RNAi	VDRC GD24068	hairpin RNA against Osm6 gene expressing under UAS promoter	
tub-GFP-Lamp1	FBrf0207605	GFP-lamp1 fusion protein expressed under the ubiquitous (tubulin) driver	[6]
Punt-GFP	VDRC 318264	Carries a fosmid genomic fragment in which punt has been fused in-frame at its C-terminus to superfolder GFP	
UAS–GFP–αTubulin	BDSC7253	GFP-αTubulin fusion expressing under UAS promoter	
Spin RNAi	TRiP.JF02782	hairpin RNA against spinster gene expressing under UAS promoter	

UAS-Spin	BDSC39668	Overexpression of spin gene used for RNAi rescue	
Lamp1 RNAi (Line1)	TRiP.HMS01802	hairpin RNA against lamp1 gene expressing under UAS promoter	
Lamp1 RNAi (Line2)	TRiP. GLV21040	hairpin RNA against lamp1 gene expressing under UAS promoter	
UAS-Dpp-mCherry		Dpp-mCherry fusion expressing under UAS promoter	[27]
Dpp-GFP	VDRC 318464	Carries a fosmid genomic construct in which Dpp has been fused in-frame to GFP	[21]
UAS-Tkv-mCherry		Tkv-mCherry fusion expressing under UAS promoter	[27]
UAS-Tkv-GFP		Tkv-GFP fusion expressing under UAS promoter	[27]
TRiP control line	BDSC35785	hairpin RNA against mCherry expressing under UAS promoter	

Genotypes used in this study. VDRC; Vienna Drosophila Resource Center, BDSC; Bloomington Stock Center.